The nature of the water nucleation sites on TiO_2(110) surfaces revealed by ambient pressure x-ray photoelectron spectroscopy

Guido Ketteler[1], Susumu Yamamoto[2], Hendrik Bluhm[3], Klas Andersson[2,4], David E. Starr[3], D. Frank Ogletree[1], Hirohito Ogasawara[2], Anders Nilsson[2,4], Miquel Salmeron[1,]*

[1] Lawrence Berkeley National Laboratory, Materials Sciences Division, Berkeley, CA94720, USA

[2] Stanford Synchrotron Radiation Laboratory, SLAC, 2575 Sand Hill Road, Menlo Park, CA94025, USA

[3] Lawrence Berkeley National Laboratory, Chemical Sciences Division, Berkeley, CA94720, USA

[4] FYSIKUM, Stockholm University, AlbaNova University Center, S-10691 Stockholm, Sweden.

[*]Corresponding author. Email: mbsalmeron@lbl.gov

ABSTRACT. X-ray photoelectron spectroscopy at ambient conditions of pressure (up to 1.5 Torr) and temperature (265K<T<800K) was used to study the adsorption of water on rutile TiO_2(110) under conditions of thermodynamic equilibrium. It was found that OH groups in bridging positions, normally present in small amounts due to residual O-vacancies, act as nucleation sites for subsequent water adsorption. The adsorption enthalpy of water binding to these sites is ~70 kJ/mol, much stronger than that in the bulk liquid (45 kJ/mol). A model is proposed that relates the structure of the oxide surface to its hydrophilic character.

Although wetting phenomena play a crucial role in environmental, chemical and biological processes, the bonding structure of water at interfaces is poorly understood. Simple questions such as the amount of

adsorbed water in equilibrium with the vapor and the structure of the first layers in contact with the surface, including the possibility of dissociation into H and OH groups remain largely unanswered. Oxides are among the most environmentally relevant materials. Rutile TiO_2 in particular is one of the most extensively studied, particularly its (110) surface [1,2]. The photochemical production of hydrogen from water and the photoinduced hydrophilicity of TiO_2 have attracted attention for potential applications [3,4]. Wet-electron states that are crucial in redox processes and charge transfer at the water interface have been characterized [5]. Changes in the electronic structure due to defects are of particular importance for water chemistry on TiO_2. The dissociation of water molecules at bridging vacancy sites has been directly imaged by STM and AFM [6,7,8,9] in ultra-high vacuum (UHV). However, these defects may not be present in solution or under ambient conditions (relative humidity 10-100%). Despite extensive efforts to characterize the interaction of water with TiO_2(110), important questions such as the nature of the sites that nucleate water adsorption and whether the molecule dissociates as a prerequisite for further adsorption remain controversial. Many experimental studies suggest that on the clean and defect-free TiO_2(110) surface water does not dissociate [1,2,6,7,10], in contrast to theoretical calculations [11,12,13]. A surprisingly long Ti-O bond length has been reported based on photoelectron diffraction [14] and interpreted as evidence for molecular adsorption, as supported by a recent calculation [15]. The current disagreement between experiments and theory may be due to the existence of high activation barriers that hinder dissociation and molecular rearrangement [16], raising the question of whether equilibrium is reached in low temperature and high vacuum studies.

Less is known about the evolution of water films thicker than a monolayer. Recent theoretical work indicates that the disorder of the H-bonded film increases and H-bonding coordination decreases as the coverage increases beyond the first and second molecular layers [17].

To address these problems we performed experiments under conditions of pressure and temperature near the ice-liquid-gas phase boundary using a specially designed Ambient Pressure Photoelectron Spectrometer.

With this instrument, x-ray photoelectron spectroscopy (XPS) could be performed under gas-surface equilibrium conditions of up to several Torr.[18].

The measurements were performed at beamline 11.0.2 of the Advanced Light Source (ALS) of the Lawrence Berkeley National Laboratory. The surface of a rutile single crystal with (110) orientation was prepared by Ar^+ sputtering (1.5 keV) followed by annealing to 900 K in vacuum and cooling to below 450 K in 10^{-5} Torr of oxygen. Measurements at relative humidity (RH) above 25% were performed using a sample holder with a Peltier element that could cool down to 250 K. With this holder the sample could not be heated to elevated temperatures and in that case the surface was prepared by Ar^+ sputtering (0.5 keV for 3 min.) followed by 30 minutes exposure to 10^{-5} Torr oxygen at room temperature. During XPS experiments the amount of adsorbed water was varied either by changing the temperature at fixed pressure (isobars) or by changing the pressure at fixed temperature (isotherms).

Different types of oxygen species (lattice O, OH, and H_2O) can be distinguished by their different O1s binding energies. With reference to the lattice oxygen peak at 530.5 eV, a peak at 1.1-1.6 eV higher binding energy appears upon exposure to water vapor, peak A in figure 1b, that is typical of hydroxyl groups at bridging sites [19,20]. These OH groups are thought to be acidic in character and to easily donate H (Brønsted acid) [20]. Oxygen-containing carbon compounds (e.g., CO, CO_2, acetone, alcohols, etc.) from background contamination can also produce a peak at this energy, particularly after filling the chamber with water vapor in the mTorr range for several minutes. The contamination originates most likely from CO and CO_2 , observed in the mass spectra acquired at water vapor pressures of 1 Torr using a differentially pumped mass spectrometer, and from hydrocarbons containing COx groups. The increase in the partial pressure of these gases is likely due to the reaction and displacement of molecules from the chamber walls upon exposure to water vapor in the torr pressure range, or from molecules contained in the water vapor itself. Indeed even after thorough cleaning to less than 1 ppm concentration, contaminants may produce 10^{-6} Torr partial pressures when the total pressure is in the Torr range. Their contribution (submonolayer amounts) was determined by using the experimentally determined ratio of O to C 1s peak areas in gas phase CO,

together with the area of adsorbed carbon to estimate, and subtract, the contamination contributions to the surface O1s peaks. The increase of a C1s peak centered around 289eV (which is typical for, e.g., O-containing organic molecules such as carboxyl, keto- or ester groups) correlates with the increase of peak A.

With further water exposure a second peak appears at 2.4 - 3.5eV higher binding energy (peak B), which can be attributed to either "basic" hydroxyl [20], or to molecularly adsorbed water [21] on Ti^{+4} sites between bridging O rows. As we shall discuss below we find no indication of hydroxyl groups on these sites. However, we can not exclude that species B could correspond to the recently proposed "pseudo-dissociated" water [6], i.e., dissociation of a water molecule into an OH group on a Ti site and a neighboring OH_{bridge}, followed by back reaction to form a water molecule.

We used the Ti2p core level to determine the vacancy concentration by using the Ti^{3+}/Ti^{4+} ratio under consideration of the electron mean free path [22] and analyzer geometry as described in Ref. [23]. The coverage of OH and H_2O was determined by measuring the areas under peaks A and B calibrated using the reference system O(2x1)/Cu(110), which has a coverage of 0.5 ML. The O1s/Cu3p peak area ratio was measured and compared with that of the O peaks on TiO_2(110) under identical experimental conditions (1 Torr of water) (see supporting information online). A monolayer (ML) on TiO_2(110) is defined as one molecule per unit cell ($5.2x10^{14}/cm^2$). Photoelectron diffraction effects were investigated in each case. We determined that they could produce an error in the absolute coverage of at most 20%. Beam induced damage (e.g., water dissociation [24]) was negligible, as determined by comparing spectra obtained after less than 6s beam exposure with spectra obtained after extensive exposure, or by comparison of irradiated and non-irradiated surface areas after exposure to water. For the photon flux in these experiments, 4×10^{14} to 3×10^{15} s^{-1} cm^{-2} at 735eV, we can estimate the x-ray induced electron dose to be below 0.1-0.3 e / water molecule. We also found no changes in the VB defect states and the defect-related Ti2p shoulder during irradiation, excluding a possible photon-induced reduction of the TiO_2 sample. Valence band (VB) spectra were normalized to the same intensity beyond the Fermi edge and at 18 eV, which is well above the O2s level. A similar approach has been used previously [25]. A full set of O1s and Ti2p spectra for the

stoichiometric, defective (0.125ML vacancies), hydroxylated and hydrated TiO_2(110) surface can be found in the supporting information online. These spectra also show that defective surfaces (0.125 ML as estimated from the shoulder of the Ti2p core level) produce a peak at about 1 eV higher binding energy than the oxide O1s core level which is not present in stoichiometric surfaces. This can only be due to O atoms neighboring the vacancy site. As we will show below and in the supporting information online, almost all vacancies are immediately healed so that there is no contribution from vacancies to the O1s core level in our experiments.

A small concentration of O-vacancy defects ($\leq$ 0.125 ML) was found to be always present after surface preparation, even after cooling in O_2. They give rise to shoulders in the low binding-energy side of the Ti^{4+} $2p_{3/2}$ peak due to reduced Ti species. Fig. 1a shows a comparison of the $Ti2p_{3/2}$ peak after sputtering (to artificially increase the amount of O vacancies), before and after exposure to water. The $Ti^{+3,+2}$ shoulder decreased very rapidly after exposure to 0.1 mTorr of H_2O, while peak A, due to hydroxyl groups, increased to a coverage of around 0.25 ML. This indicates that most of the vacancy defects are readily filled, except for a very small residual amount (< 0.03 ML), which we attribute to bulk defects [2]. A hydroxyl coverage of 0.25 ML is indeed expected from the initial 0.125 ML of vacancies present in this case, if each water molecule dissociates into an OH group that fills the vacancy, and a H atom that forms an identical species by binding to another bridging O site. For defect concentrations lower than 0.125 ML, the final OH coverage is also lower, but always equal to twice the defect concentration. The following experiments were performed on a surface with an initial defect concentration of 0.125 ML.

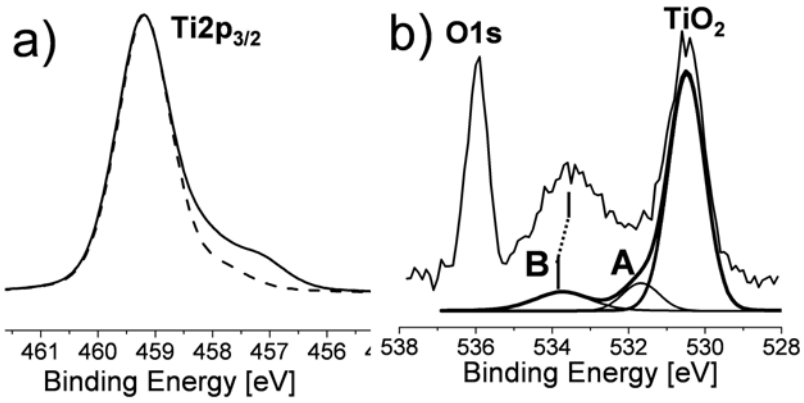

Fig. 1: (a) $Ti2p_{3/2}$ XPS peak of Ar-sputtered TiO_2(110) at 420 K before water exposure (solid line) and after introduction of 0.1 mTorr of H_2O (dashed line). Photon energy 630 eV. (b) O1s XPS spectrum in the presence of 17 mTorr H_2O at 298 K (bottom curve), and 1 Torr at 270K (top curve). Photon energy 690 eV. Peaks A and B correspond to OH and molecular water, respectively. Only peak B changes with water exposure, increasing in intensity and shifting to lower energies. The peak at 536 eV corresponds to gas phase water.

To ascertain the existence of thermodynamic equilibrium between vapor and surface we performed isobar and isotherm experiments. The isobar in fig. 2a, recorded in 0.4 Torr water, shows that the OH coverage is constant over the temperature range from 800K to 275K and equal to twice the initial defect concentration. Water adsorbs on the OH-saturated surface until its coverage equals that of the OH groups. After this, as the temperatures decreases, the water coverage increases more rapidly. Qualitatively similar results were obtained from isotherms, as shown by the room temperature data set in fig. 2b. As expected from equilibrium measurements both curves collapse into one when the data are plotted as a function of relative humidity (RH), as shown in fig. 2c. The RH is defined as $p/p_v(T)\times 100$, where p_v is the equilibrium vapor pressure of bulk water or ice at the corresponding temperature.

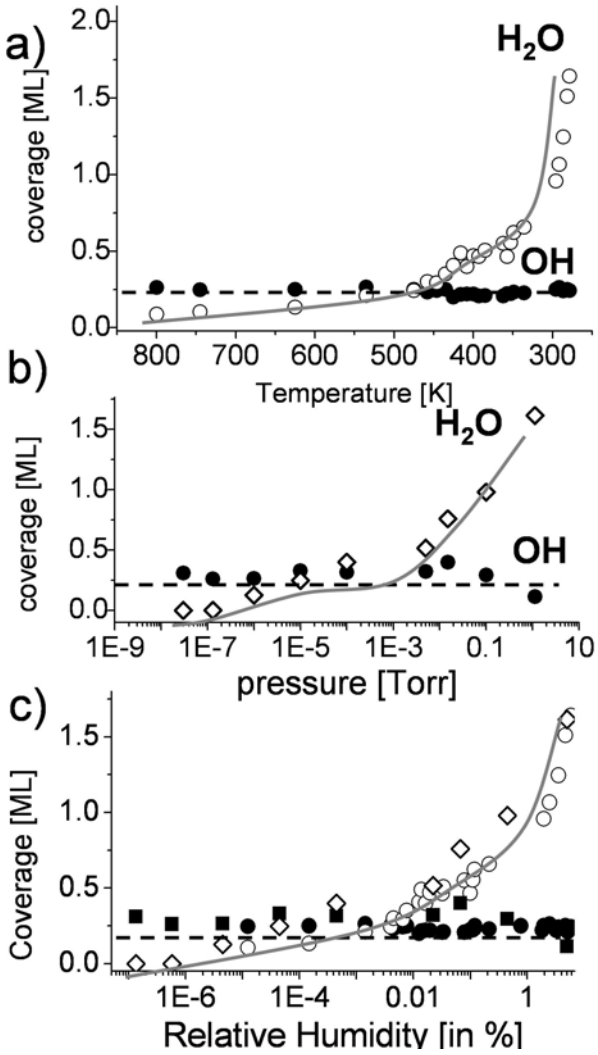

FIG 2: (a) Isobar (p = 0.4 Torr) and (b) Isotherm (T = 298 K) showing the water and OH coverage as a function of decreasing temperature and increasing pressure, respectively. (c) Same data plotted as a function of relative humidity. Empty diamonds and filled squares: Isotherm; Filled and empty circles: Isobars. Both results collapse into the same curve, demonstrating that the surface and gas phase are in thermodynamic equilibrium. Dashed and solid lines are inserted as a visual aid.

Fig. 3a shows the variation of OH and water coverage over a wide range of relative humidity. The coverage of water (from peak B in fig. 1b) increased rapidly between 0 and 25% RH, with inflections at approximately 12 and 25% RH, which correspond to 2 ML and 3 ML, respectively. Between 25 and 50-60% RH water coverage changed slowly, and then increased rapidly when approaching 100% RH. As before, the amount of bridging OH species remained constant at twice the initial defect concentration (~0.25 ML). Details of the growth of the first water monolayer can be better followed in the enlarged plot of fig.

3b, which summarizes the results of three different experimental isobars. As can be seen, from $5x10^{-5}$ %RH to $3.5x10^{-3}$ %RH (cooling the sample from 800 to 475 K in the presence of 0.4 Torr of water) the amount of adsorbed water increases up to a coverage equal to the initial OH coverage (~0.25 ML), where the uptake curve shows an inflexion followed by a small plateau. Between 0.25 ML and 2 ML water coverage, the O1s XPS peak of adsorbed water shifts towards lower binding energies by 0.5 eV (fig. 4), with most of the shift taking place below 1 ML.

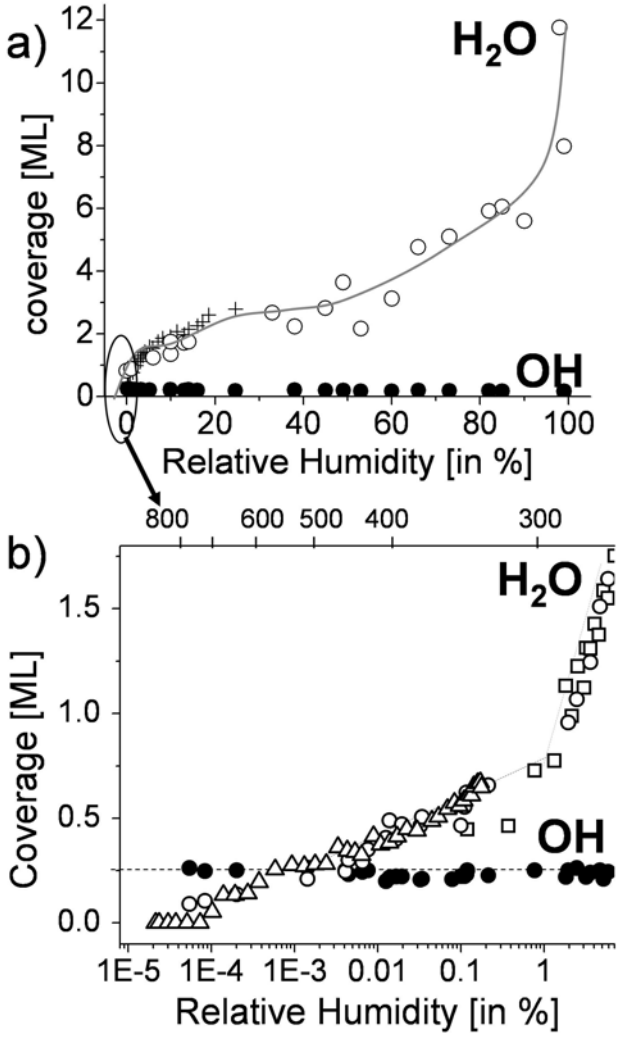

Fig. 3: (a) Coverage of OH and H_2O obtained from different isobars (10^{-2} to 1.5 Torr) as a function of relative humidity (RH). Cross symbolds are data obtained with the heater sample holder and large dots with the Peltier sample holder. (b) Enlarged view of the low relative humidity region (data from three different isobars: open triangles and filled circles, 0.01 Torr; empty circles, 0.4 Torr; empty squares, 1Torr). The temperature scale at the top corresponds to the 0.4 Torr isobar. Notice the change of the x-axis from linear to logarithmic in the two plots. There is a plateau at 0.25 ML in (b), when the coverage of water equals that of OH.

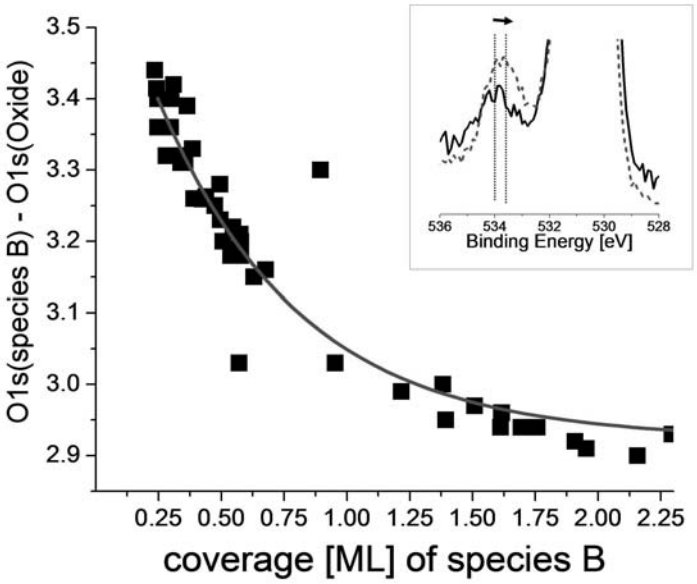

Fig. 4: O1s core level shift of species B (H_2O) relative to the lattice oxygen peak as a function of coverage. A shift to lower binding energy is observed above $\theta = 0.25$ ML. The inset shows two spectra under 17 mTorr of H_2O corresponding to low and high coverage.

The temperature dependence of the coverage from several isobars was used for an isosteric determination of the adsorption enthalpy and entropy of water [26]. For each coverage the equilibrium pressures and temperatures were plotted in the form *ln* p vs. 1/T (fig. 5), following the Clausius-Clapeyron equation. Since the gas and surface temperatures are not the same in isobar experiments the use of the Clausius-Clapeyron equation is not strictly valid. However, it is easy to show that the error incurred is very small. This is due to the fact that equilibrium is determined by the equality of the rate of adsorption of gas molecules on the surface, which varies as $p/\sqrt{T}$, and the rate of desorption, which varies as $\exp(-E/kT)$. It is clear that it is the surface temperature that is by far the most important. The maximum error when using $T_{surface}$ instead of T_{gas} for the adsorption rate occurs at $T_{surface} = 850$ K at which point it is 3.3 kJ/mol. Other sources of error are likely more important. For example, the temperature and pressure during data acquisition varied on the order of <5%, so that average values were used in the plot. Straight line fits to these plots were used to calculate the enthalpy (slope) and entropy (y-axis intercept) of adsorption. As can be seen they vary with coverage. The obtained values are shown in fig. 6, with the error bars representing the statistical deviation

from the fits. The error due to the p,T variations shown in fig. 5 is difficult to quantify and is not included in this figure. In particular, the entropy values might be affected by this and figure 6b shows a more qualitative trend. The enthalpy shows a minimum of -72 kJ/mol at 0.25 ML (fig. 6). For higher coverage the adsorption energy is close to the enthalpy of condensation of liquid water (-45 kJ/mol). The entropy shows a small minimum around 0.3 ML but overall remains close to ~70 J/Kmol, which corresponds to the entropy of liquid water. The thermodynamic properties of the adsorbed film above 0.25 ML rapidly approach those of liquid water.

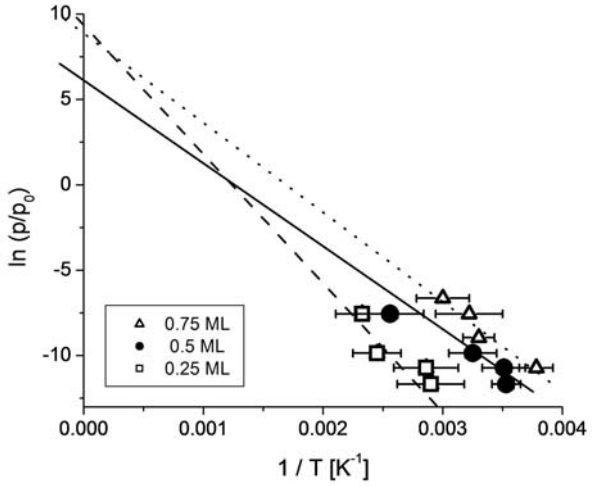

FIG 5. Isosteric *ln p* vs. *1/T* plots of data from different isobars corresponding to a coverage of 0.25 ML (open squares), 0.5 ML (filled symbols), and 0.75 ML (open triangles). The slope of the best fit represents the enthalpy of adsorption for this coverage, and the y-intersection corresponds to the entropy. The bars represent variations in the pressure and temperature and the uncertainty of the peak fit.

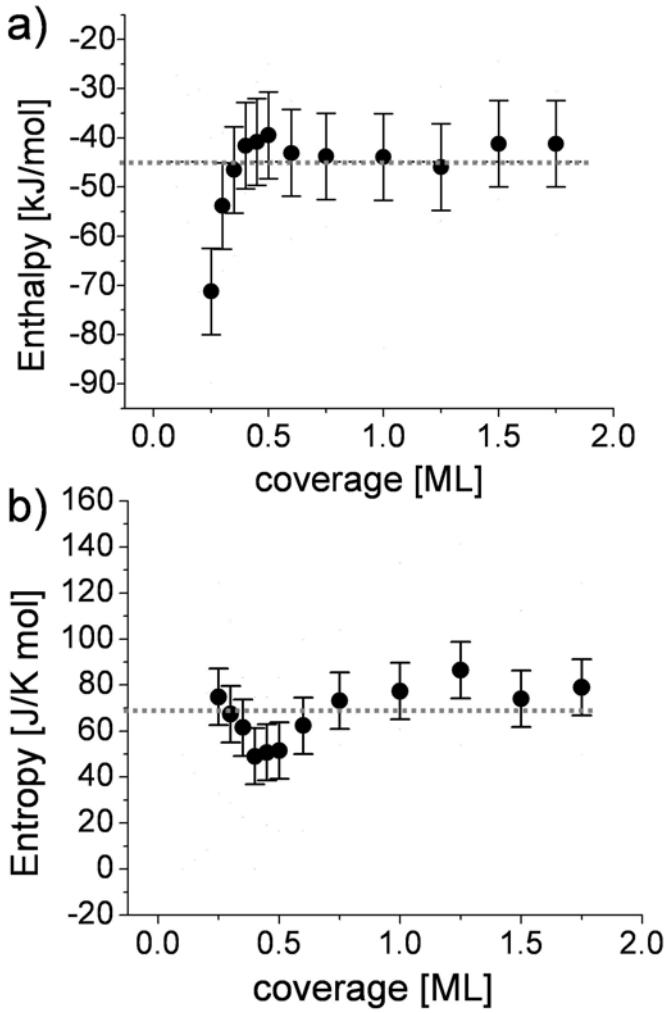

FIG 6. (a) Enthalpy and (b) entropy of adsorbed water as a function of coverage obtained from isosteric measurements. The dotted horizontal lines indicate the enthalpy and entropy for liquid water. Below 0.25 ML the error bar is too large for accurate determination of the slope. Statistical error bars for the best fit results from fig. 5 are included. Note that there might be an additional error due to the p,T variations displayed in fig. 5 (in particular for the entropy).

Our observations can be explained with the following model. First water dissociates at O-vacancies in bridge sites, producing a stoichiometric amount of OH bridge groups equal to twice the initial vacancy concentration: $H_2O + V_{bridge} + O_{bridge} = 2OH_{bridge}$ This step takes place even at very low humidity. Water is then adsorbed molecularly, bonding to these OH groups that act as H-donors. Possible H_2O_{ads}-H_2O_{ads} interactions between these OH-H_2O complexes can not be excluded. The -72 kJ/mol adsorption enthalpy of water for the 1:1 OH_{bridge}:H_2O ratio (fig. 6) compares well with the activation energy for water desorption at

270-295K derived from thermal desorption spectroscopy [21,27]. The sharp decrease of enthalpy towards the value of bulk water above 0.25 ML shows that the OH_{bridge} groups create very favorable adsorption configurations for water and that only after they are saturated do new H_2O adsorption configurations appear. It has been suggested from XPS data [19] that species B, which we attribute to molecularly adsorbed water, could be due to basic hydroxyl groups on fivefold coordinated Ti sites. However this implies dissociation of H_2O, a process that would produce a hydrogen atom that should react with oxygen atoms to form additional OH_{bridge} groups. We do not observe an increase in the OH_{bridge} coverage.

In summary, we have shown that water adsorption occurs in distinct steps. First oxygen vacancies dissociate water and become hydroxylated even at very low water pressure. We found that such bridge O-vacancies are normally present even if only in small amounts on the most carefully prepared surfaces (e.g., annealed in O_2). These vacancies are filled with OH by water dissociation even in high vacuum. These OH_{bridge} groups act as a Brønsted acid sites that anchor water molecules to form strongly bound OH-H_2O complexes. These then act as nucleation centers for further water adsorption. As more water attaches to these nucleation centers, the acidic character of the adsorption complex decreases and the water binding structure tends to that of the bulk liquid. This is achieved after adsorbing approximately 2 ML of water. The kink at 2 ML coverage suggests the formation of a water or ice bilayer at 12% relative humidity, which needs to be confirmed by microscopic measurements. The thermodynamic properties of the adsorbed water film on TiO_2(110) are similar to liquid water. The wetting properties of TiO_2(110) are thus driven by moderate amounts (<0.25 ML) of strongly attractive OH sites that nucleate an H-bonded liquid-like water layer.

ACKNOWLEDGMENTS. This work was supported by the Director, Office of Science, Office of Biological and Environmental Research and the Chemical Sciences Division of the U.S. Department of

Energy under Contract No. DE-AC02-05CH11231, and by the NSF-CHE-0089215 grant. GK thanks the Alexander-von-Humboldt foundation for financial support.

References

[1] M.A. Henderson, Surf. Sci. Rep. **46**, 1 (2002).

[2] U. Diebold, Surf. Sci. Rep. **48**, 53 (2003).

[3] R. Wang, K. Hashimoto, A. Fujishima, M. Chikuni, E. Kojima, A. Kitamura, M. Shimogoshi, T. Watanabe, Nature **388** , 431 (1997).

[4] K. Honda and A. Fujushima, Nature **238**, 37 (1972).

[5] K. Onda, B. Li, J. Zhao, K.D. Jordan, J. Yang, H. Petek, Science **308**, 1154 (2005).

[6] S. Wendt, J. Matthiesen, R. Schaub, E.K. Vestergaard, E. Lægsgaard, F. Besenbacher, B. Hammer, Phys. Rev. Lett. **96**, 066107 (2006).

[7] S. Wendt, R. Schaub, J. Matthiesen, E.K. Vestergaard, E. Wahlstrom, M.D. Rasmussen, P. Thostrup, L.M. Molina, E. Lægsgaard, I. Stensgaard, B. Hammer, F. Besenbacher, Surf. Sci. **598**, 226 (2005).

[8] O. Bikonda, C. L. Pang, R. Ithnin, C.A. Muryn, H. Onishi, G. Thornton, Nature Mat. **5**, 189 (2005).

[9] C.L. Pang, A. Sasahara, H. Onishi, Q. Chen, G. Thornton, Phys. Rev. **B74**, 073411 (2006).

[10] I.M. Brookes, C.A. Muryn, G. Thornton, Phys. Rev. Lett. **87** , 266103 (2001).

[11] P.J.D. Lindan, N.M. Harrison, M.J. Gillan, Phys. Rev. Lett. **80** , 762 (1998).

[12] K. Jug, N.N. Nair, T. Bredow, Surf. Sci. **590**, 9 (2005).

[13] A. Fahmi, C. Minot, Surf. Sci. **304**, 343 (1994).

[14] F. Allegretti, S. O'Brian, M. Polcik, D.I. Sayago, D.P. Woodruff, Phys. Rev. Lett. **95**, 226104 (2005).

[15] L.A. Harris, A.A. Quong, Phys. Rev. Lett. **93**, 086105 (2004).

[16] P.J.D. Lindan, C. Zhang, Phys. Rev. **B72** , 075439 (2005).

[17] C. Zhang, P.J.D. Lindan, J. Chem. Phys. **119**, 9183 (2003).

[18] D.F. Ogletree, H. Bluhm, G. Lebedev, C.S. Fadley, Z. Hussain, M. Salmeron, Rev. Sci. Instrum. **73**, 3872 (2002).

[19] L.-Q. Wang, D.R. Baer, M.H. Engelhard, A.N. Shultz, Surf. Sci. **344** , 237 (1995).

[20] T.K. Sham, M.S. Lazarus, Chem. Phys. Lett. **68** , 426 (1979).

[21] M.B. Hugenschmidt, L. Gamble, C.T. Campbell, Surf. Sci. **302,** 329 (1994).

[22] M.P. Seah, W.A. Dench, Surf. Interface Anal. **1**, 2 (1979).

[23] L.-Q. Wang, D.R. Baer, M.H. Engelhard, Surf. Sci. **320**, 295 (1994).

[24] K. Andersson et al., Phys. Rev. Lett. **93**, 196101 (2004).

[25] R.L. Kurtz, R. Stockbauer, T.E. Madey, E. Roman, J.L. de Segovia, Surf. Sci. **218**, 178 (1989).

[26] W. Ranke, Y Joseph, Phys. Chem. Chem. Phys. **4**, 2483 (2002).

[27] D. Brinkley, M. Dietrich, T. Engel, P. Farrall, G. Gantner, A. Schafer, A. Szuchmacher, Surf. Sci. **395**, 292 (1998).